ARTICLE

Comparison Between Large-Eddy Simulation and Reynolds-Averaged Navier–Stokes Computations for the MUST Field Experiment. Part II: Effects of Incident Wind Angle Deviation on the Mean Flow and Plume Dispersion

A. Dejoan · J. L. Santiago · A. Martilli · F. Martin · A. Pinelli

Received: 22 December 2008 / Accepted: 21 January 2010

Abstract Large-eddy simulations (LES) and Reynolds-averaged Navier–Stokes (RANS) computations of pollutant dispersion are reported for the Mock Urban Setting Test (MUST) field experiment flow. In particular we address the effects of incident wind angle deviation on the mean velocity and on the mean concentration fields. Both computational fluid dynamical methods are assessed by comparing the simulation results with experimental field data. The comparative analysis proposes to relate the plume deflection with the flow channelling effects. The results show that the plume deflection angle varies with the altitude. As the ground is approached the plume is shown to be almost aligned with the street canyon direction and independent of the incident wind directions considered. At higher altitudes well above the obstacles, the plume direction is aligned with the mean wind direction as in dispersion over flat terrain. The near-ground plume deflection is the consequence of a strong channelling effect in the region near the ground. The mean concentration profiles predicted by LES and RANS are both in good qualitative agreement with experimental data but exhibit discrepancies that can be partly explained by the influence of small incident wind angle deviation effects. Compared to RANS, LES predicts a higher channelling and thus a higher deflection of the plume. Results on the fluctuating intensity of the concentration obtained from LES show a satisfactory agreement with experiments. This information is not available from RANS for which only the mean concentration modelling is considered.

Keywords Channelling effects · Large-eddy simulation · MUST experiment · Reynolds-averaged Navier–Stokes · Plume deflection

A. Dejoan · A. Pinelli
Energy Department, Research Center for Energy, Environment and Technology (CIEMAT),
Av. Complutense 22, 28040 Madrid, Spain

J. L. Santiago (✉) · A. Martilli · F. Martin
Environment Department, Research Center for Energy, Environment and Technology (CIEMAT),
Av. Complutense 22, 28040 Madrid, Spain
e-mail: jl.santiago@ciemat.es

1 Introduction

Dispersion of contaminants in the urban environment is far more complex than dispersion in open terrain. Unlike that for flat terrain, the direction of the plume can be deflected from the main wind direction under the influence of high flow channelling within the building array. Flow channelling occurs when the upstream wind direction deviates from the normal direction to the front of the obstacles and depends on the incident wind angle deviation. Yee and Biltoft (2004) observed that at relatively small obliquity of the flow incidence (i.e. for an incidence angle smaller than 20° measured with respect to the normal direction to the front of the array) the plume centreline direction is deflected towards the normal to the front of the array, while at a higher incidence angle the mean plume centreline direction is deflected away from the normal to the front direction. The plume centreline deflection was investigated in the Mock Urban Setting Test (MUST) field experiment using a RANS formulation by Milliez and Carissimo (2007) and with very large-eddy simulation (VLES) by Camelli et al. (2005). Experiments on the influence of wind direction on the mean flow pattern and channelling effects were carried out in a simplified urban environment by Cole et al. (2006). In particular, they considered the effects of the wind approach angle and building spacing on the flow over a restricted number of obstacles in a water channel. Making use of RANS computations, Kim and Baik (2004) classified different mean flow patterns depending on the wind direction and related them to the spatial distribution of passive pollutant through a regular matrix of cubical obstacles.

As a continuation of Part I (Santiago et al. 2010), the present study aims to compare RANS and LES approaches. However, while in Part I the comparisons focused only on flow properties, both approaches are here assessed for the simulation of pollutant dispersion. The grid resolution used for the LES has the same characteristics as that used in Part I, i.e. it ensures a reasonable resolution of the large obstacle-related flow scales while maintaining computational times that do not exceed two orders of magnitude those needed by the RANS simulations. Again, the MUST flow configuration (Biltoft 2001) is used for the comparisons. This configuration is similar to that termed the "irregular case" as described in detail in Part I, but with the difference that the incident flow is not directed perpendicular to the front of the array but is at some oblique incident angle. The proposed comparative study is based on an analysis of the local flow channelling effects on the pollutant dispersion that includes the effects of a small deviation of the angle of the flow incident direction. These effects are addressed by considering one trial of the MUST experimental dataset (one mean incident flow direction angle and one release) and by providing an analysis of the sensitivity of the pollutant dispersion to small angle variations from the mean incident wind direction, of the order of the standard deviation reported in the trial. The flow channelling and the small angle variation effects are locally analysed, i.e. at different altitudes from the ground. Previous studies on the plume deflection or on the flow channelling (Milliez and Carissimo 2007; Camelli et al. 2005) did not provide detailed information. Note that the atmospheric conditions corresponding to the experimental data sample used for the comparisons are near-neutral so that neutral conditions are assumed in the present simulations. Also, as in the experiment, the pollutant is a passive one.

The paper is organised as follows: the computational set-up is described in Sect. 2, and results are presented in Sect. 3 as follows. First, a qualitative overview of the pollutant plume dispersion is given in Sect. 3.1; secondly, the mean concentration profiles are compared with the experiments (Sect. 3.2); thirdly, an analysis of the flow channelling effects on the plume dispersion is given in Sect. 3.3, which includes comparisons of the deflection angle of the flow from the incident mean wind direction between RANS, LES and experiments. In Sect. 3.4

Journal: 10546-BOUN Article No.: 9467 MS Code: BOUN573.3 TYPESET DISK LE CP Disp.:2010/1/30 Pages: 18 Layout: Small

a comparison between the LES results obtained for the fluctuating concentration field and experimental data is presented. Finally, some concluding remarks are given in Sect. 4.

2 Computational Set-Up Description

2.1 Numerical Modelling of the Pollutant Concentration

The LES and RANS methodologies used for the computation of the flow field are described in detail in Part I (Santiago et al. 2010). Here, we will mainly focus on the models used for the computation of the pollutant concentration.

In LES, the concentration evolution is given by the filtered passive scalar equation

$$\frac{\partial \widetilde{C}}{\partial t} + \frac{\partial \widetilde{U}_j \widetilde{C}}{\partial x_j} = D \frac{\partial^2 \widetilde{C}}{\partial x_j \partial x_j} - \frac{\partial \sigma_j}{\partial x_j} \tag{1}$$

where $\widetilde{C}$ is the filtered concentration, D is the scalar diffusivity and $\widetilde{U_j}$ is the filtered velocity component. The subgrid-scale scalar stress σ_j is modelled via an eddy gradient diffusion hypothesis as,

$$\sigma_j = -\frac{\nu_{sgs}}{Sc_{sgs}} \frac{\partial \widetilde{C}}{\partial x_j} \tag{2}$$

where ν_{sgs} is the subgrid-scale viscosity and Sc_{sgs} defines the turbulent subgrid-scale Schmidt number.

Regarding the RANS methodology, the evolution of the mean concentration is given by a transport equation for a passive scalar very similar to Eq. 1, in which the filtered flow quantities have to be replaced by the mean flow quantities. The scalar stress is similarly modelled as in LES, i.e. via the diffusion gradient hypothesis:

$$\sigma_j = -\frac{\nu_t}{Sc_t} \frac{\partial \overline{C}}{\partial x_j} \tag{3}$$

where ν_t is the turbulent viscosity expressed as $\nu_t = C_\mu k^2/\varepsilon$ and Sc_t is the turbulent Schmidt number. Here, C_μ(=0.09) is a model constant and k and ε are the turbulent kinetic energy (TKE) and the dissipation rate of TKE, respectively.

The computation of pollutant dispersion is influenced by the Schmidt number values. Here, we fix the Schmidt numbers to the most commonly used values in order to maintain the turbulence and subgrid-scale models in their most general form. The Schmidt number is set to 0.6 in the LES simulations according to Neto et al. (1993). In the RANS simulations it is set to 0.9, a value widely used with the k–ε model for the computation of dispersion in an urban environment (Kim and Baik 2004; Santiago et al. 2007; Tominaga and Stathopoulos 2007). Both values rely on the physical background that a passive pollutant is transported with a similar effectiveness as momentum. Note that the correspondence between the RANS and LES Schmidt numbers is not straightforward as the turbulent diffusion is partly explicitly resolved in LES while it is fully modelled in RANS.

The numerical schemes used in the LES to resolve the concentration equation is similar to those used for the flow field equations, except that, for the convective terms, the bounded total variation scheme (Jasak 1996) was used in order to maintain the concentration values positive. In the RANS calculations the numerical scheme of the concentration equation is identical to that used for the flow equations.

Journal: 10546-BOUN Article No.: 9467 MS Code: BOUN573.3 TYPESET DISK LE CP Disp.:2010/1/30 Pages: 18 Layout: Small

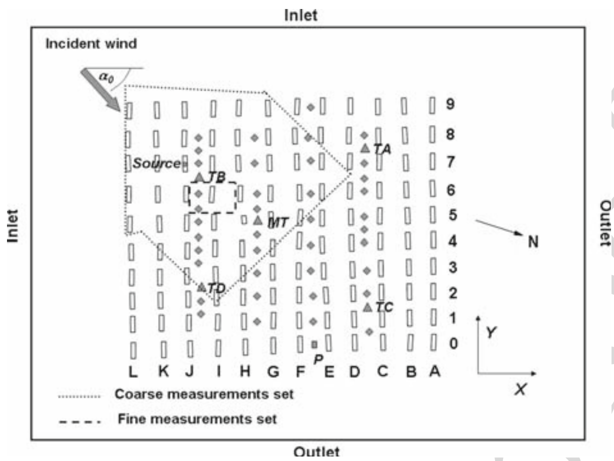

Fig. 1 Plan view of the MUST field geometry. *Triangles* towers, *circle* pollutant source, *square* location P; *diamond* probe locations at $z/h = 0.63$

2.2 Flow Geometry and Parameters

The flow geometry is identical to the MUST field experiment that was described in detail in Part I. The experimental release data base chosen for the simulations corresponds to the trial 2682353 of the measurements campaign (Yee and Biltoft 2004). The propylene gas tracer used in the experiments was released with a sampling time of approximately 15 minutes. In order to alleviate the unsteady effects inherent in real meteorological conditions, the least mean variation of the wind speed and direction were extracted over samples of 200 s from the 15 minutes of release data. This procedure allows for undertaking comparisons among the trial data, simulation results and wind-tunnel experimental measurements (see Yee et al. 2006).

The array forms an angle of 30° with the north direction as shown Fig. 1. For the considered trial (see trial 16, Table II of Yee and Biltoft 2004), it is reported that, at the altitude $z = 4$ m, the incident wind direction angle, α_0 (see Fig. 1), measured at the upwind mast takes the mean value of $-47°$ with a standard deviation of 7.5°. By computing the mean incident wind direction at the other altitudes available from the sample measurements we found that the wind direction also changes slightly with height, with a variation of the mean angle within the range [$-47°$ to $-50°$] when moving from $z = 4$ m to $z = 16$ m. Finally, by taking into account the angular variations with altitude z, the value of the mean incident wind direction angle extracted is $\alpha_0 = -48°$. Note that, here, the wind direction is defined by reference to the normal front of the obstacles (see Fig. 1) and that this reference system will be used afterwards.

In the RANS simulations, three incident wind direction angles are considered, $\alpha_0 = -42°$, $-48°$ and $-54°$. Due to the higher computational time required compared for RANS, only the results obtained with the two angles $\alpha_0 = -42°$ and $-48°$ are presented for the LES. Note that this angle range covers the mean value of the incident wind angle extracted from the sample data ($\alpha_0 = -48°$) and two values that are representative of the standard deviation from the mean incident wind direction reported in the selected experiment trial.

The Reynolds number, $Re = U_0 h/\nu$ (based on the maximum incident wind speed, U_o, the height of the container, h, and the kinematic viscosity, ν) is similar to that of the field

Journal: 10546-BOUN Article No.: 9467 MS Code: BOUN573.3 TYPESET DISK LE CP Disp.:2010/1/30 Pages: 18 Layout: Small

experiments ($Re = 10^6$). Regarding the size and grid resolution, the computational domain is identical to that used in Part I for the irregular case.

In the LES, the statistical concentration data were extracted from one pollutant release realization (once the flow is fully developed) and calculated over a long time period of release that corresponds to approximately 12 large-eddy characteristic time scales.

2.3 Boundary Conditions

The boundary conditions for the flow are similar to those used in the irregular case of Part I. In both RANS and LES, the mean inflow velocity profiles are extracted from a power-law profile that matches the measurements given at a mast located upstream of the array of obstacles. The obtained profiles are applied to the horizontal velocity components at the inlet boundaries of the computational domain (see Fig. 1). The RANS turbulent kinetic energy at the inlet is interpolated from the experimental data and the dissipation profile deduced from the equilibrium hypothesis. In the LES, the inlet turbulent fluctuations are represented by random noise.

The release of the pollutant is simulated by adding a local source term (S_C) to the right-hand side of Eq. 1 at the trial release position (i.e. on the roof of the container J7, see Fig. 1). The value of the source term is applied over one computational cell and is such that the value of the imposed flux corresponds to the experimental value, $Q = 3.75 \times 10^{-3}\,\mathrm{m}^3\,\mathrm{s}^{-1}$. For the pollutant we used zero-gradient boundary conditions at the surface of the containers and at the top, bottom and outflow boundaries.

3 Results

As already mentioned, one particular experimental trial (number 2682353) of the MUST field campaign was chosen for the comparisons between the LES and RANS simulations. First, an overview of the pollutant plume dispersion is given. Then, the profiles of the mean concentration are compared between RANS, LES and the experimental field data (Yee and Biltoft 2004). Later on, an analysis of the flow channelling effects on the plume deflection is presented and a comparison made of channelling-related flow quantities (profiles of mean angle deviations as a function of the distance from the ground) with the MUST wind-tunnel experimental data (Bezpalcova 2007; Leitl et al. 2007) corresponding to a flow configuration with a close inlet wind direction ($\alpha_0 = -45°$) is provided. Note that, for this angle, the wind-tunnel experiment did not include measurements of the pollutant dispersion corresponding to a source comparable to that in the selected trial. Finally, the LES results obtained when considering fluctuating concentration intensity are compared with the experimental data of Yee and Biltoft (2004). As mentioned in the Introduction, the modelling of the fluctuating concentration was not taken into account in the present RANS calculation.

3.1 Overview of the Plume Behaviour

Figure 2a and b provides iso-contours of the pollutant mean concentration over the full computational domain in the plane $z/h = 0.63$, obtained with both LES and RANS for the incident wind direction angle set at $\alpha_0 = -48°$. Superposed on the iso-contours are three ranges of the mean concentration extracted from the experimental data at the four horizontal lines of sampling stations located at $z/h = 0.63$ and shown in Fig. 1. This allows for providing a qualitative overview of the pollutant plume dispersion. It is shown that the spread of the plume

Journal: 10546-BOUN Article No.: 9467 MS Code: BOUN573.3 TYPESET DISK LE CP Disp.:2010/1/30 Pages: 18 Layout: Small

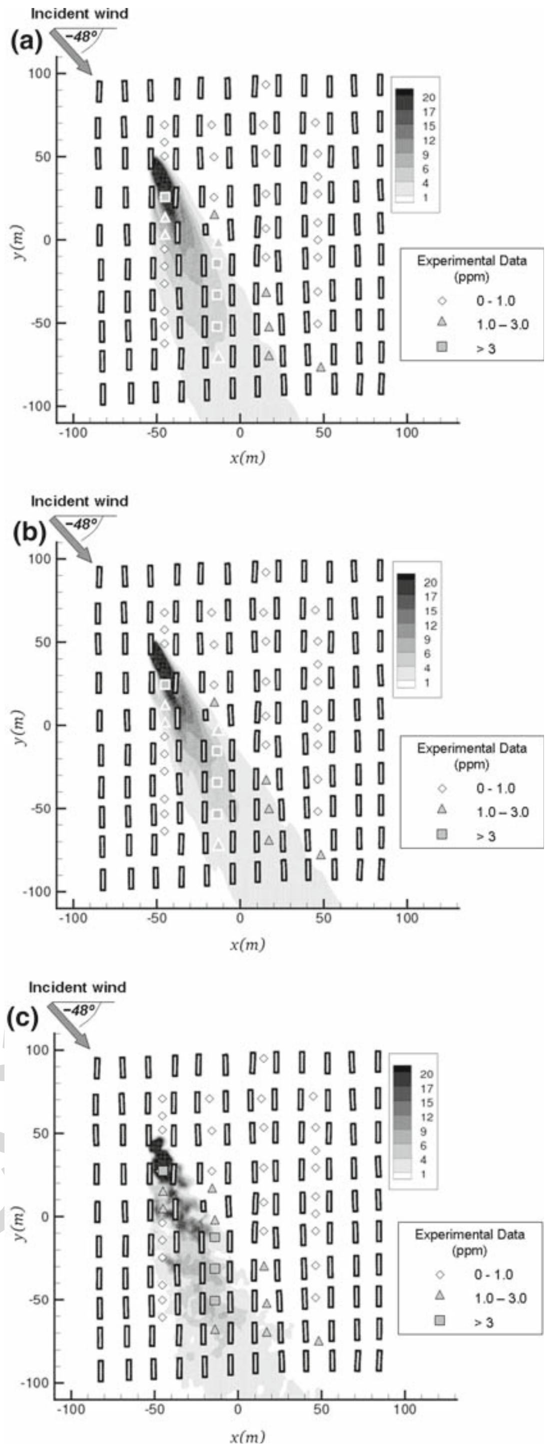

Fig. 2 **a** Isocontours of the pollutant mean concentration at $z/h = 0.63$ for the wind direction angle $\alpha_0 = -48°$ obtained from LES simulations; **b** As in **a** but for RANS simulation; **c** Instantaneous snapshot of the isocontours of the concentration at $z/h = 0.5$ for the wind direction angle $\alpha_0 = -48°$ obtained from LES. *Symbols with white contours* indicate the probe locations used for the comparison in Fig. 5

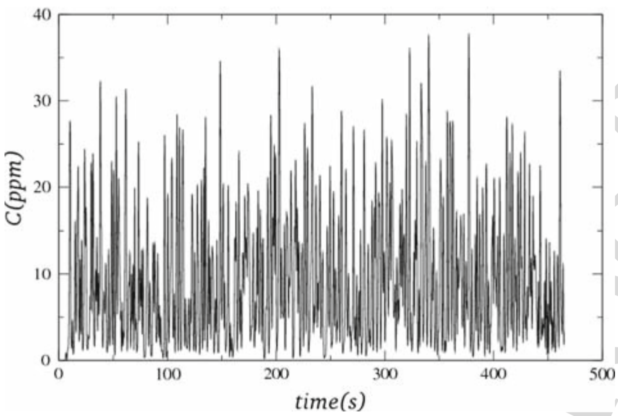

Fig. 3 Time evolution of the instantaneous concentration obtained from LES at the location ($x = -45.5$ m, $y = 14.84$ m, $z = 1.6$ m, see Fig. 2c) for an incident wind direction angle $\alpha_0 = -48°$

given by the RANS and LES is in satisfactory agreement with the experimental data. Some differences are observed between RANS and LES, in particular the line defining the edge of the plume suggests a higher deflection of the plume predicted by LES. At the plume edge, the concentration presents high fluctuations around relatively low mean values, as is illustrated in Fig. 2c; this shows the iso-contours of a snapshot of the instantaneous concentration field obtained with LES at the same altitude, $z/h = 0.63$, as in Fig. 2a. Note that strong concentration fluctuations are present within the plume as shown in Fig. 3, where the time evolution of the instantaneous LES concentration is given at the location ($x = -46$ m, $y = 15$ m).

3.2 Mean Concentration Profiles

The vertical mean concentration profiles obtained from LES and RANS are compared with experimental data at the locations of the meteorological towers reported in Fig. 1: the main tower (MT) located near the centre of the obstacle array, the tower B (TB) located in the south-west quadrant, and the towers C (TC) and D (TD) located in the north-east and south-east quadrants, respectively. Tower A was not taken into account for the comparison because it is located beyond the zone spanned by the plume (see Figs. 1 and 2).

The mean concentration profiles are shown in Fig. 4a and d for the incident wind angles $\alpha_0 = -42°$, $-48°$ and $-54°$ for RANS and $\alpha_0 = -42°$ and $-48°$ for LES. Note that the standard deviation of the concentration was added to the LES profiles to give an idea of how the concentrations fluctuate around the mean value for each considered angle. A good overall qualitative agreement is observed between the mean concentration profiles obtained from LES and RANS and the experimental data. Indeed, at all the tower locations and for all the incident angles considered, the simulation profiles exhibit a similar shape to the one given by the experimental data. However, quantitative discrepancies between the experiments and the simulations are observed. The agreement with the measurement is shown to depend on the location and on small-angle deviations of the incident wind direction, which makes it difficult to draw definite conclusions about the comparative performance of RANS and LES. In particular, at tower TB both RANS and LES overestimate the concentration for any angle α_0, LES results being somewhat closer to the experimental data. At tower TD, the RANS provides a better agreement with the measurements for $\alpha_0 = -42°$ and $-48°$ while LES tends, in general, to overestimate the mean concentration. At the two other locations, MT and

Journal: 10546-BOUN Article No.: 9467 MS Code: BOUN573.3 TYPESET DISK LE CP Disp.:2010/1/30 Pages: 18 Layout: Small

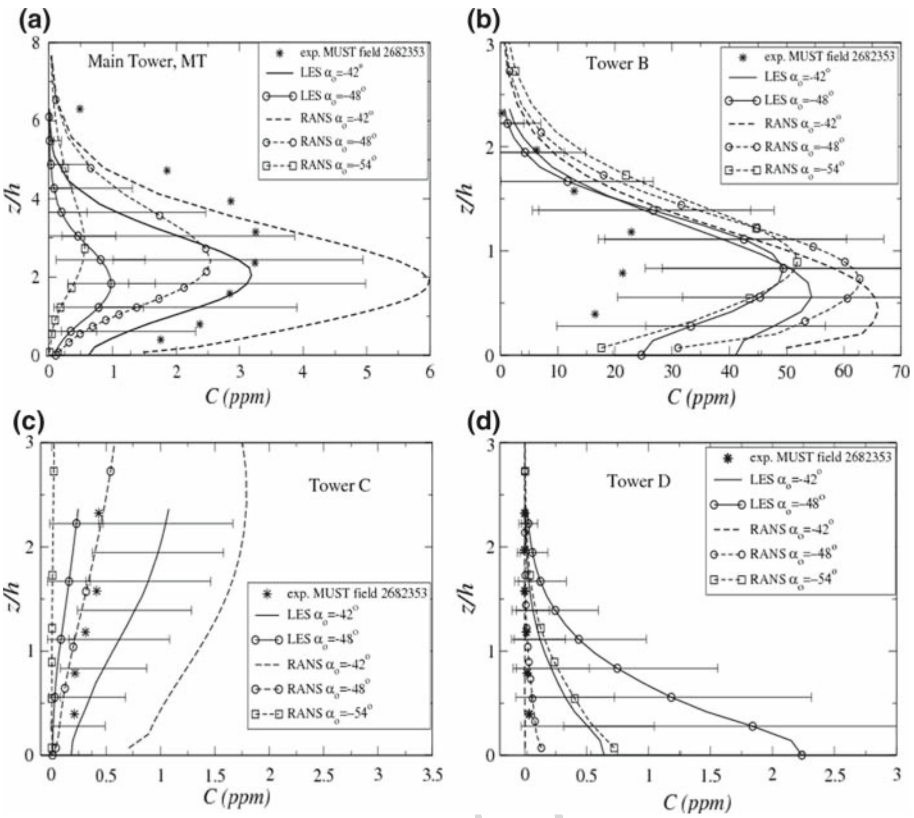

Fig. 4 Mean concentration vertical profiles given at: **a** main tower, **b** tower B, **c** tower C and **d** tower D. *Horizontal bars* indicate the standard deviation of the concentration obtained in LES simulations

TC, RANS (for $\alpha_0 = -48°$) and LES (for $\alpha_0 = -42°$) give results close to the experimental data. Note that tower TB is located close to the source so that the overestimation given by RANS and LES can be explained by a lack of local grid refinement around the location of the pollutant release. At towers MT, TC and TD, the mean concentration is shown to be very sensitive to small deviations of the incident wind direction. These towers are located close to the edge of the plume where the horizontal gradients of concentration are strong. In this region, a small change of wind direction determines whether the probe locations are outside or inside the plume, with changes in the concentration of more than 100%. At tower TB, well within the plume, the effects of incident angle variations are less important. To complete the comparisons, Fig. 5 provides the mean concentrations obtained by RANS and LES for $\alpha_0 = -42°$ and $\alpha_0 = -48°$ put side by side with the measurements at several probe locations located within the plume at $z/h = 0.63$ (shown in Fig. 2). It is shown that, close to the release location, the mean concentration is overestimated (a possible consequence of the lack of grid resolution around the point source) but that for distances from the source $d/h > 20$ (where d is defined in Fig. 5), both RANS and LES agree well with the experimental data. The effects of small deviations of the incident wind direction are observed to be lower (in relative values) than the ones previously shown on the vertical profiles of the mean concentration at the near edge of the plume (see Figs. 4 and 5). This suggests that part of the discrepancies

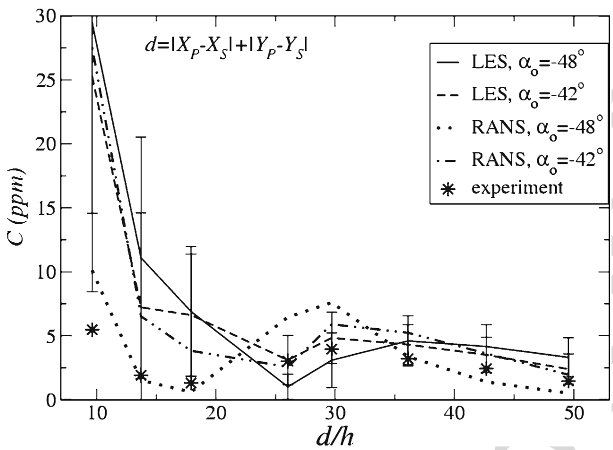

Fig. 5 Mean concentration along eight probes located in the core of the plume at $z/h = 0.63$ (see Fig. 2). *Vertical bars* indicate the standard deviation of the concentration obtained in LES simulations. Note that X_S and Y_S are the *x*- and *y*-coordinates of the source and X_P and Y_P the *x*- and *y*-coordinates of the probe locations shown Fig. 2a and b

found with the experiments at the probe locations far from the release and close to the border of the plume (MT, TC and TD) can be attributed to the fluctuating character of the incident wind direction in real atmospheric conditions. LES and RANS simulations performed with a smaller angle deviation (of 2°) showed a similar behaviour for the mean concentration (not shown here). Note that, taking into account the standard deviation of the concentration, the LES mean concentration values cover globally the range of RANS and experimental data at the selected locations.

When considering flat terrain, the plume deflection is easier to predict than in an urban environment. Indeed, a deviation of the mean wind direction in flat terrain will produce an equal deviation of the mean plume direction. However, in an urban environment the plume deflection depends on several factors such as the geometry of obstacles, the aspect ratio of the streets, and the locations of the point sources, so that the spread and shape of the plume are strongly influenced by the complex flow inside the urban canopy. New questions arise about the feature of flow channelling inside the array and about the influence of small deviations of the incident wind direction on pollutant dispersion in the urban environment. These issues are addressed in the next section.

3.3 Flow Channelling and Plume Deflection

3.3.1 Channelling Effect

The neutral character of the pollutant considered in this study ensures that the plume dispersion is mainly governed by the flow velocity field. Thus, the deflection of the pollutant plume can be mainly related to the flow channelling. To illustrate this flow feature, we computed the horizontal spatial average of the time mean deviation angle, defined as the difference between the flow direction and the inlet wind direction angles, $\langle \Delta\overline{\alpha} \rangle = \langle \overline{\alpha} \rangle - \alpha_0$. The spatially-averaged flow direction angle, $\langle \overline{\alpha} \rangle$, is obtained from the ratio of the tangential time mean velocities averaged over horizontal planes covering the entire array of containers, $\langle \overline{V} \rangle / \langle \overline{U} \rangle$. The vertical profiles of the absolute value of $\langle \Delta\overline{\alpha} \rangle$ extracted from the LES and RANS data

Journal: 10546-BOUN Article No.: 9467 MS Code: BOUN573.3 TYPESET DISK LE CP Disp.:2010/1/30 Pages: 18 Layout: Small

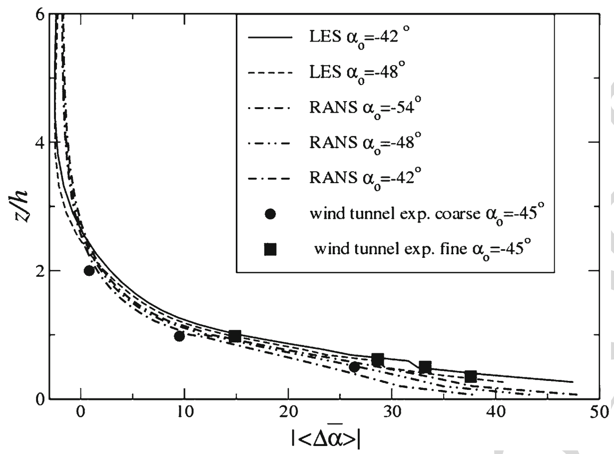

Fig. 6 Vertical profiles of the spatial-average time-mean deviation angle, $|\langle\Delta\overline{\alpha}\rangle|$

are given in Fig. 6 for the mean incident wind angles $\alpha_0 = -42°$ and $\alpha_0 = -48°$. These results are compared with the deviation angle obtained from the wind-tunnel experimental data performed by Bezpalcova (2007) and Leitl et al. (2007) for an incident wind angle $\alpha_0 = -45°$. Two sets of experimental data were used from the available velocity measurements to obtain the spatial average of the flow direction angle. One set corresponds to the spatial averages of measurements performed over a zone representing about 30% of the full domain (covering, approximately the lines of obstacles L9-L5,K9-K5, J9-J4, I9-I3, H9-H4, G9-G5, F8-F6 and E7, see Fig. 1). This set will be referred as the "coarse measurements set". The other experimental dataset used for comparison corresponds to measurements performed with a better resolution than the coarse measurements set but covering a reduced part of the domain (from the lines J6-J5 to H6-H5 approximately), and will be referred as the "fine measurements set". Figure 6 shows a good agreement between the two experimental datasets and the RANS and LES predictions. As in the experiment, the profiles of $\langle\Delta\overline{\alpha}\rangle$ is found to exhibit a lateral deflection of the flow relative to the mean incident wind direction that increases as the ground is approached: i.e. the flow is observed to be deflected away from the normal to the front of the array as height diminishes. This behaviour corroborates the observations on plume deflection reported by Yee and Biltoft (2004) for the obliquity of the incident wind higher than 20°. Close to the ground the average wind direction is shown to be almost aligned with the *y*-direction, which indicates that the flow is highly channelled in this region. As *z/h* increases, the channelling effects decrease and for $z/h > 3$ the deviation of the mean flow direction from the incident wind direction becomes almost negligible. LES and RANS give close results, LES predicting a slightly more pronounced deflection. Note that the $\langle\Delta\overline{\alpha}\rangle$ profiles exhibit a weak dependence on the incident wind direction angle for the cases presented here. Although not shown here, the alignment of the wind direction with the *y*-direction as the ground is approached was also observed in LES and RANS simulations performed with an incident wind angle $\alpha_0 = -30°$.

The flow channelling can also be analysed locally by providing the profiles of the time mean deviation angle, $|\Delta\overline{\alpha}|$, at some probe locations. Figure 7 gives the deviation angle profiles obtained with RANS and LES for $\alpha_0 = -48°$ at the two tower locations MT and TB, and also at a third location P, positioned within the region of the containers placed close to the exit of the domain (see Fig. 1). The $|\Delta\overline{\alpha}|$ profiles are similar to those of $|\langle\Delta\overline{\alpha}\rangle|$; however

Journal: 10546-BOUN Article No.: 9467 MS Code: BOUN573.3 TYPESET DISK LE CP Disp.:2010/1/30 Pages: 18 Layout: Small

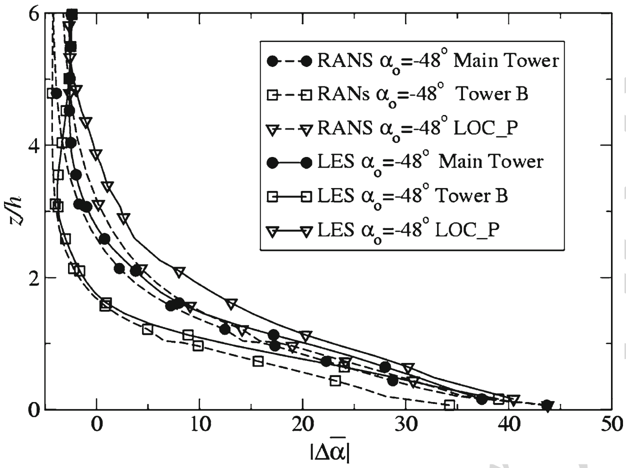

Fig. 7 Vertical profiles of the time-mean deviation angle, $|\langle\Delta\alpha\rangle|$, at the main tower, tower B and at location P (see Fig. 1) for $\alpha_0 = -48°$

it is clear that, for a given incident wind direction, the mean deviation depends on the spatial location. The deflection tends to be stronger as the flow spans further inside the array: when moving from tower TB to location P, the mean deviation is observed to increase; again, although not shown here, similar profiles were obtained for $\alpha_0 = -42°$. The LES and RANS simulations predict similar results, however, the flow channelling is stronger in the LES than in the RANS. This behaviour, already suggested by the higher plume deflection observed in LES than in RANS (see Sect. 3.1 and Fig. 2a, b), becomes more evident when considering the representation of the streamlines drawn at the horizontal planes located at $z/h = 0.5$ and $z/h = 0.2$ given in Fig. 8a–d for RANS and LES, respectively. Figure 8c and d clearly shows that both numerical approaches predict an almost perfect alignment of the flow direction with the y-direction as the ground is approached. Also, note that the recirculation eddies predicted by the RANS at the altitude $z/h = 0.2$ are larger along the x-direction, which may explain the lower deflection of the flow as compared to the LES results. The spatial dependence of the mean flow direction implies a spatial dependence of the passive pollutant dispersion and thus explains that, for a given incident wind direction, the centreline direction of the plume dispersion will depend on the release location, a behaviour previously observed by Milliez and Carissimo (2007) in their RANS calculations.

The present results show that the mean flow direction near the ground inside the array appears to be mainly governed by the array configuration (orientation of the containers) rather than the incident wind direction. Obviously, this makes a great difference in comparison with the case of flow over flat terrain where a change in the wind direction produces a deviation of the flow in the whole domain. The plume dispersion is thus expected to be less influenced by the mean incident wind direction in the urban environment (depending on the altitude from the ground) than in open terrain. This feature is addressed in the next section.

3.3.2 Plume Deflection

In order to gain insight into how the plume is deflected within the array, we present the isolines of the pollutant concentration extracted from the horizontal planes $z/h = 0.1$ and $z/h = 4$ and the two incident wind angles $\alpha_0 = -42°$ and $\alpha_0 = -48°$, for both LES and RANS

Journal: 10546-BOUN Article No.: 9467 MS Code: BOUN573.3 TYPESET DISK LE CP Disp.:2010/1/30 Pages: 18 Layout: Small

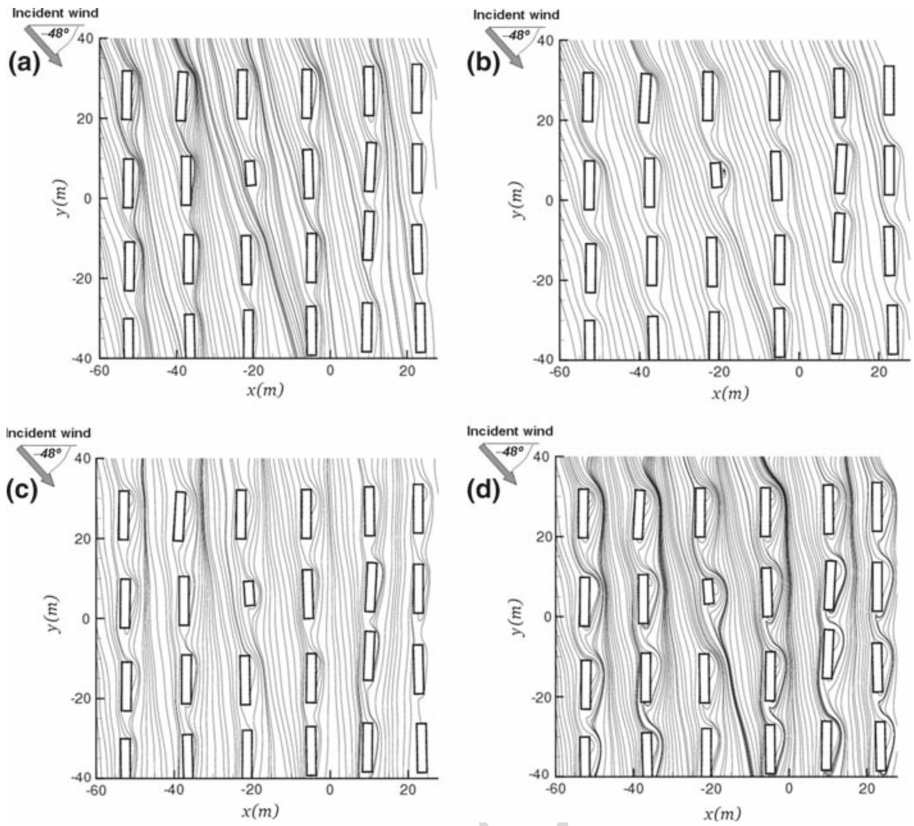

Fig. 8 Streamlines of the mean flow velocity field for $\alpha_0 = -48°$: **a** LES at $z/h = 0.5$, **b** RANS at $z/h = 0.5$, **c** LES $z/h = 0.2$ and **d** RANS at $z/h = 0.2$. Note that the 2D representation of the streamlines corresponds to the lines tangential to the velocity vector field projected in the corresponding plane

simulations in Fig. 9a and b, respectively. Each isoline corresponds to 50% of the maximum concentration in each plane.

Figure 9a and b shows that the plume deflection predicted by LES and RANS is almost insensitive to the change in the direction of the upwind flow at $z/h = 0.1$ while at $z/h = 4$ the effect of the incident wind direction angle is clear. This corroborates the previous analysis on the flow channelling, which showed that very near to the ground the flow direction is almost aligned with the *y*-direction independently of the incident wind direction. Well above the obstacles the plume does not interact with the obstacles and follows the main incident wind direction. Thus, compared to dispersion in flat terrain where the plume, being aligned with the main wind direction, shows a high sensitivity to small deviations of the approaching wind direction and propagates in the same direction independently of the altitude, the orientation of the plume within an array of obstacles varies with height. The present results suggest as well that the dispersion of a pollutant released at ground level will be less sensitive to deviations of the incident wind direction than the dispersion of a pollutant emitted at higher altitudes. This behaviour is illustrated by Fig. 9c, which represents the isolines of concentration in the same way as for Fig. 9a and b but for a RANS calculation performed with a pollutant

Journal: 10546-BOUN Article No.: 9467 MS Code: BOUN573.3 TYPESET DISK LE CP Disp.:2010/1/30 Pages: 18 Layout: Small

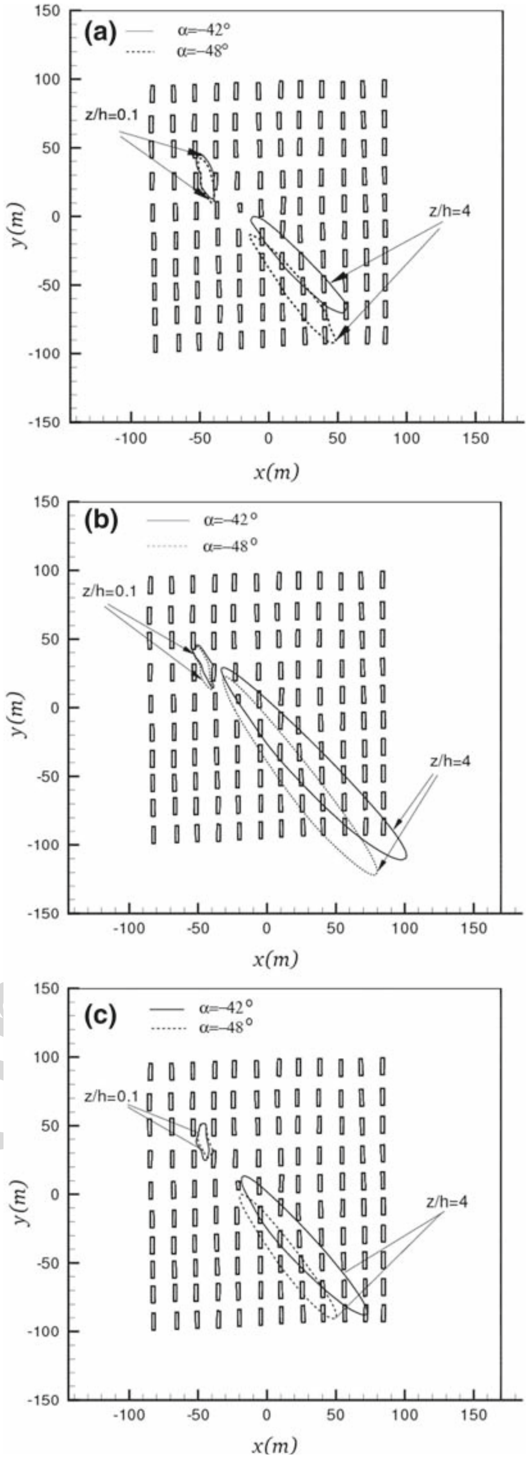

Fig. 9 Pollutant concentration isolines given at the horizontal planes $z/h = 0.1$ and 4 for the two incident wind angles −42° and −48°: **a** LES simulations with the release above the roof, **b** same as **a** but for RANS simulation, **c** same as **b** but for a pollutant release located at the ground level between two containers. The isolines corresponds to 50% of the maximum concentration value in each plane

Journal: **10546-BOUN** Article No.: **9467** MS Code: **BOUN573.3** TYPESET DISK LE CP Disp.:**2010/1/30** Pages: **18** Layout: **Small**

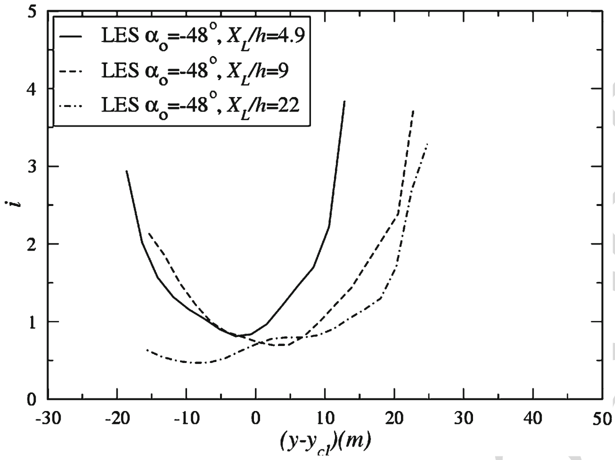

Fig. 10 LES: variations along the y-direction of the fluctuating intensity i at different normalized centreline plume downwind distances X_L/h from the source. Note that Y_{cl} defines the y-coordinate of the point located at X_L

release located at ground level. The differences of the plume direction between $\alpha_0 = -42°$ and $\alpha_0 = -48°$ at the plane $z/h = 0.1$ are indeed smaller than those shown in Fig. 9b.

The differences between LES and RANS for the plume direction are hardly discernible in Fig. 9a and b and are clearer from Fig. 2a and b, showing that LES predicts a higher deflection plume than RANS. This tendency is in agreement with the stronger flow channelling found in the LES simulations (see Sect. 3.1).

3.4 Fluctuation Concentration Field

The fluctuation of the concentration field is generally characterized by the fluctuating intensity parameter, i, defined as $i = \sigma/\overline{C}$, where σ is the standard deviation given by $\sigma = ((C - \overline{C})^2)^{1/2}$, with C being the instantaneous concentration and $\overline{C}$ the mean concentration.

Figure 10 gives the lateral evolution of the fluctuating intensity along the y-direction at different downwind locations from the source along the mean plume centreline, X_L/h, at $z/h = 0.63$. As observed by Yee and Biltoft (2004), on the lateral cross-sections the fluctuating intensity increases when approaching the edge of the plume while it reaches minimum values at the mean plume centreline. At the edge of the plume, the concentration presents large fluctuations but relatively low mean values so that the intensity may be high in this region. The cross-sections of the evolution of the intensity are almost symmetric along the mean plume centreline. The slight differences observed in the values of the intensity between the two edges for a given distance X_L/h are mainly due to the non-orthogonality of the centreline direction of the plume with the y-direction. For $X_L/h = 22$, this effect is enhanced by the higher lateral deflection of the plume as the domain exit is approached (see Fig. 7a and related comments). Note that this effect was not taken into account when defining the distances X_L/h (evaluated along a mean line originating from the source).

The evolution of i along the normalized downwind plume centreline distance X_L/h is shown in Fig. 11 at different normalized heights from the ground, z/h, for the incident wind direction angle $\alpha_0 = -48°$. A comparison with the experimental data of Yee and Biltoft (2004) obtained for $z/h = 0.63$ and for a range of values of the mean incident flow direction

Journal: 10546-BOUN Article No.: 9467 MS Code: BOUN573.3 TYPESET DISK LE CP Disp.:2010/1/30 Pages: 18 Layout: Small

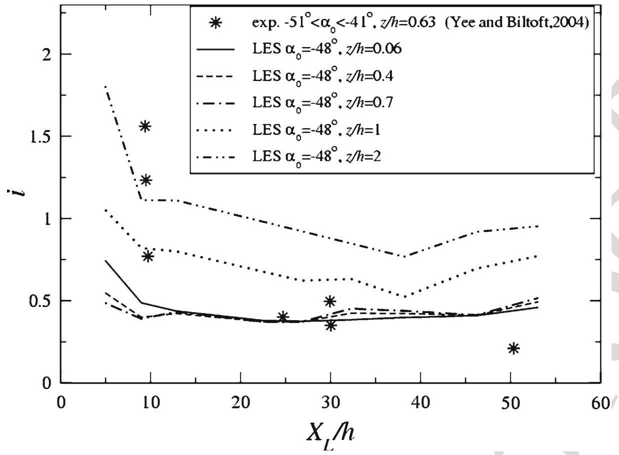

Fig. 11 LES: variation of the fluctuating intensity *i* along the normalized centreline plume downwind distance X_L/h from the source, given at altitudes *z*/*h*

angle that surrounds the value $\alpha_0 = -48°(-51° < \alpha_0 < -41°)$ is also given. Note that the experimental values of the incident wind angle are given in our reference system according to Fig. 8 of Yee and Biltoft (2004). The experimental data of the fluctuating intensity were extracted from Fig. 13 of Yee and Biltoft (2004) and correspond to different source locations. However, Yee and Biltoft (2004) showed that, for distances located well downwind of the source, the fluctuating intensity tends to "forget" the initial source conditions as the plume is subject to a continuous mixing process within the canopy so that these data can be used for the present comparison. A satisfactory agreement is found between the LES predictions and the experimental data. In particular the intensity displays a peak in the region close to the pollutant release location, decaying further downstream to reach a value that is close to the measurements for downwind distances from the source $X_L/h > 10$ and for altitudes $z/h < 1$. Close to the source location the simulations tend to underestimate the intensity. This can be explained by a combination of a lack of local grid refinement and an effect of the source conditions in this zone as mentioned above. The simulations show that the intensity is lower within the canopy than in the upper layer, which is in agreement with a stronger mixing process within the canopy arising from high-intensity turbulence generated by the containers.

The vertical profiles of the fluctuating intensity at several locations along the centreline plume direction are given in Fig. 12. In agreement with Yee and Biltoft (2004), the fluctuating intensity increases rapidly as the upper edge of the plume is approached and is lower in the canopy layer. The experimental data used for comparisons are extracted from Fig. 11 of Yee and Biltoft (2004); they correspond to a flow incidence angle of $\alpha_0 = -10°$ and were measured at the location $X_L/h = 18$ from the source location. The incident wind direction of this experimental set is different from that for the simulations. However, the LES provides intensity profiles in quite good agreement with measurements within the canopy layer. It is interesting to note that the fluctuating intensity in this region is almost insensitive to the incident wind direction. This is in agreement with the small angle effects reported in this region (see Sect. 3). Above the canopy (for distances $z/h > 2$) the concentration intensities are higher than the experimental data and significantly dependent on the direction angle α_0. A possible explanation for the differences observed above the canopy is related to the use

Journal: 10546-BOUN Article No.: 9467 MS Code: BOUN573.3 TYPESET DISK LE CP Disp.:2010/1/30 Pages: 18 Layout: Small

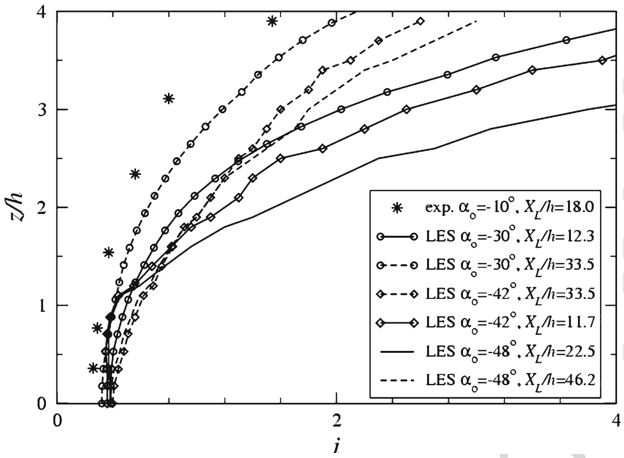

Fig. 12 LES: vertical profiles of the fluctuating intensity i given at different normalized plume centreline downwind distance X_L/h

of random noise to represent the turbulence fluctuation at the inlet. This may result in a lower pollutant transport through turbulence diffusion so that the mean concentration may be underestimated and thus the fluctuating intensity overestimated. However, Fig. 4 shows that, well above the containers, the LES predicts satisfactory mean concentration levels. Another explanation is that the selected locations X_L/h are computed at the given altitude $z/h \approx 0.63$ (as in the experiment) and thus do not include the variation of the mean plume direction with height. As z/h increases, the plume direction tends to recover the incident wind direction so that strong angle effects are expected in this region. This is confirmed by the LES results obtained for $\alpha_0 = -30°$, which show that when the incident wind direction approaches the experimental one a better agreement with the measurements is obtained.

4 Conclusions

In the present study we compared RANS with LES considering a grid resolution that ensures simultaneously a reasonable resolution of the large scales of flow motions generated by the obstacles and relatively moderate computational times for the simulation of the MUST field experiment for passive pollutant dispersion. The comparative analysis included the study of the effects of small angle deviations of the incident wind direction on the mean concentration field obtained from the simulations, and as well addressed the relevance of these effects on the flow channelling and the plume dispersion. The performance of LES for the prediction of pollutant dispersion was also assessed by comparing the LES-predicted fluctuating concentration field data with experimental data. This information was not available in the present RANS calculations for which the modelling of the fluctuating concentration was not included.

Both present RANS and LES predictions of the mean concentration are found to be both in good overall qualitative agreement with the experimental data. At locations close to the edge of the plume the quantitative discrepancies observed can be partly explained by large effects of small fluctuations of the incident wind direction in this bounding region. In the core of the plume, LES and RANS give similar results that are in reasonable quantitative

Journal: 10546-BOUN Article No.: 9467 MS Code: BOUN573.3 TYPESET DISK LE CP Disp.:2010/1/30 Pages: 18 Layout: Small

agreement with the measurements and the effects of small deviations from the incident wind direction are found relatively lower than those at the edge of the plume.

The analysis of the flow channelling shows that, when spatially averaged over horizontal planes covering the full array of containers, the vertical profiles of the mean deviation angles between the incident wind direction and the flow direction within the urban array predicted by the LES and RANS are very close and in agreement with the experimental data. These profiles show that the flow channelling within the array is stronger when approaching the ground where the flow is observed to be almost aligned with the *y*-direction for any incident wind angle considered. For a given incident wind direction, the local mean deflection angle shows a spatial dependence. The flow deflection is found to be stronger in the LES predictions.

As a consequence of the flow channelling effect, the plume is highly deflected in regions very close to the ground where its direction tends to align as well with the *y*-direction. In this region the plume direction is almost insensitive to small deviations of the mean incident wind direction. However, as the distance from the ground increases, the plume direction tends to align itself with the incident wind direction so that small angle deviation effects are comparable as those found in flat terrain. Finally, the fluctuating intensity of the concentration predicted by the LES is found to be in satisfactory agreement with the experimental data.

Acknowledgments The authors wish to thank J.M. White and B. Leitl for providing field data and wind-tunnel data of the MUST experiment, respectively and J. Franke for providing one of the meshes used in this study. The present study was funded by the Spanish Ministry of Defence.

References

Bezpalcova K (2007) Physical modelling of flow and dispersion in an urban canopy. PhD thesis, Faculty of Mathematics and Physics, Charles University, Prague, 193 pp

Biltoft CA (2001) Customer report for Mock Urban Setting Test (MUST). DPG document WDTC-TP-01-028, West Desert Test Center, U.S. Army Dugway Porving Ground, Dugway, Utah, 58 pp

Camelli FE, Lohner R, Hanna SR (2005) VLES Study of MUST experiment. In: 43rd AIAA Aerospace Meeting and Exhibit, January 10–13, Reno, Nevada, paper 1279

Cole T, Li X, Eising C, Princevac M (2006) Turbulence and channeling in a simple urban environment. In: AMS 17th symposium on boundary layer and turbulence, San Diego

Jasak H (1996) Error analysis and estimation for the finite volume method with applications to fluid flow. PhD thesis, Imperial College, University of London, 394 pp

Kim JJ, Baik JJ (2004) A numerical study of the effects of ambient wind direction on flow and dispersion in urban street canyons using the RNG k-epsilon turbulence model. Atmos Environ 38:3039–3048

Leitl B, Bezpalcova K, Harms F (2007) Wind tunnel modelling of the MUST experiment. In: 11th international conference on harmonisation within atmospheric dispersion modelling for regulatory purposes, Cambridge, July 2–5, UK, 5 pp

Milliez M, Carissimo B (2007) Numerical simulations of pollutant dispersion in an idealized urban area for different meteorological conditions. Boundary-Layer Meteorol 122:321–342

Neto AS, Grand D, Metais O (1993) A numerical investigation of the coherent vortices in turbulence behind a backward-facing step. J Fluid Mech 256:1–25

Santiago JL, Martilli A, Martin F (2007) CFD simulation of airflow over a regular array of cubes. Part I: three-dimensional simulation of the flow and validation with wind-tunnel measurements. Boundary-Layer Meteorol 122:609–634

Santiago JL, Dejoan A, Martilli A, Martin F, Pinelli A (2010) Comparison between Large-eddy simulations and Reynolds-averaged Navier–Stokes computations for the MUST field experiment. Part I: study of the flow when the incident wind direction is perpendicular to the array. Boundary-Layer Meteorol (in press)

Tominaga Y, Stathopoulos T (2007) Turbulent Schmidt numbers for CFD analysis with various types of flow field. Atmos Environ 41:8091–8099

Yee E, Biltoft CA (2004) Concentration fluctuation measurements in a plume dispersing through a regular array of obstacles. Boundary-Layer Meteorol 111:363–415

Yee E, Gailis RM, Hill A, Hilderman T, Kiel D (2006) Comparison of wind tunnel and water-channel simulations of plume dispersion through a large array of obstacles with a scales field experiment. Boundary-Layer Meteorol 121:389–432